




Research Article

Metamaterial inspired THz antenna for breast cancer detection

G. Geetharamani¹ · T. Aathmanesan² 

© Springer Nature Switzerland AG 2019

Abstract

Metamaterial inspired Terahertz (THz) antenna for breast cancer detection proposed in this paper. The proposed antenna consists of a simple rectangular patch configuration integrated with Complementary Split Ring Resonator (CSRR). The design equations along with the equivalent circuit and permittivity calculations also presented in this paper. The experimental technique for detection of tumor in human breast model by the simulation technique also presented. The proposed metamaterial inspired antenna operates at 1 THz frequency with 20 dBi of gain. Its design evolution process, parametric study, and results such as farfield radiations also presented in this paper.

Keywords Metamaterials · Terahertz antenna · CSRR · Breast cancer detection.

1 Introduction

Researchers around the world are working to find better ways to prevent, detect, and treat breast cancer, and to improve the quality of life of patients and survivors. Therefore, it is more significant to advance the cancer diagnostic systems for better detection and treatment. Breast cancer is one among the common cancer in which the classical approach for detection includes mammography technology which must advance with the new technology for improving the diagnosis accuracy. Therefore, in this paper a new metamaterial inspired THz antenna for breast cancer detection presented which can more accurately detect the presence of tumor in the breast tissue. A detailed study on breast cancer tumor size, overdiagnosis and mammography screening effectiveness discussed in [1]. A need for optimal breast cancer screening with personalized approach that integrates patient specific and age dependent metrics of cancer risk with selective application of specific screening technologies discussed in [2]. A combination of thermal and Electromagnetic (EM) analysis of breast cancer detection by using the surface temperature variation and perturbation concepts

discussed in [3]. A study to evaluate a phyllodes tumor of the breast with magnetic resonance imaging (MRI) and magnetic resonance spectroscopy along with a detailed case study discussed in [4]. Breast cancer detection using the microwave radar technique discussed in [5–8]. A smart antenna array-based microwave imaging system for brain cancer detection focuses on tumor position discussed in [9]. A screening system for antenna array based on microwave breast cancer detection with five antennas to identify the development of malignant tissue in the women breast discussed in [10]. A flexible mild microwave hyperthermia antenna application for chemothermotherapy of the breast discussed in [11].

A novel compact Side Slotted Vivaldi Antenna (SSVA) for microwave breast imaging discussed in [12] which includes compound radar, Integrated microwave imaging radar, Time domain multistate radar systems. The conventional medical imaging techniques uses X-rays, Magnetic resonance imaging, Ultrasound, Computer tomography and positron emission which are of low resolution and high cost for implementation and complex systems in which X-rays used in mammography for detection of breast tumor where a high false negative

✉ T. Aathmanesan, cegnesan@gmail.com | ¹Department of Mathematics, Anna University, Chennai, Tamilnadu, India. ²Department of ICE, Anna University, Chennai, Tamilnadu, India.



SN Applied Sciences (2019) 1:595 | <https://doi.org/10.1007/s42452-019-0601-6>

Received: 8 February 2019 / Revised: 2 May 2019 / Accepted: 13 May 2019 / Published online: 18 May 2019

rate of (4–34%) and high false positive rate of (70%) have reported [13]. The potential of (0.3–0.5 THz) frequencies in the cancer detection near field imager discussed in [14]. THz reflection imaging to distinguish between cancer and non-cancer breast tissue discussed in [15]. A Double Debye model to understand the dielectric response of biological tissues at THz frequencies especially at breast cancer discussed in [16]. An apparatus which can operate on 1.89 THz to locate cancer in the human breast tissue discussed in [17]. A novel microstrip patch antenna on photonic crystal in THz discussed in [18]. Analysis of photonic crystal and multi-frequency terahertz microstrip patch antenna discussed in [19]. Theoretical analysis including the acquisition speed, spatial resolution, Signal to Noise Ratio (SNR), Dynamic range, Depth of field, Noise equivalent power discussed for the state-of-the-art THz antenna technology for imaging applications discussed in [20]. The Metamaterial concept first introduced by Veselago in the year 1968 [21]. Analytical design procedure of CSRR presented along with its equivalent circuit design discussed in [22]. An experimental demonstration of optically thin metamaterial resonating in the THz regime with the 70% of maximum resonance amplitude achieved by using half skin depth thick lead (Pb) split-ring resonators (SRR) array discussed in [23]. The THz spectrum lies between Infrared (IR) and Microwave and it finds many applications in Biology, Medicine, Imaging, Security etc., and a brief review of metamaterials in THz region such as metamaterial absorbers, modulators, switches, lenses, and cloaking structures have discussed in [24].

Some state-of-the-art microwave breast cancer detection systems discussed in [6, 25–30]. A biomedical microwave tomography system with 3D-imaging capabilities and an accurate recovery of 3D dielectric property distributions for breast-like phantoms with tumor inclusions utilizing both the in-plane and new cross-plane data in [25]. A novel compound imaging approach presented to overcome these physical constraints and improve the imaging capabilities of a multistatic radar imaging modality for breast scanning applications discussed in [6]. A microwave imaging system developed as a clinical diagnostic tool operating in the 3- to 8-GHz region using multistatic data collection in [26]. A second-generation monostatic radar system to measure microwave reflections from the human breast presented and analyzed in [27]. a monostatic radar-based approach to microwave imaging and utilizes ultra-wideband signals used microwave breast imaging system used to scan a small group of patients discussed in [28]. An ultrawideband (UWB) radar-based breast cancer detection system, which is composed of complementary metal–oxide–semiconductor integrated circuits, presented in [29]. The detectability of a handheld impulse-radar breast tumor detector demonstrated

in [30]. From the literature review, there are techniques for detection of tumors in breast tissue using the microwave frequency were mostly available and the use of THz frequency is evolving gradually and the need for research in developing a THz based cancer detection system is increasing. Therefore, in this paper metamaterial inspired THz antennas for breast cancer detection presented. The organization of this paper consists of introduction with the literature review in Sect. 1 and its evolution of design along with the design methodology of the CSRR in the Sect. 2. Section 3 consists of the breast cancer detection experiment using the sample breast tissues with its results and discussion, and the Sect. 4 concludes the paper.

2 Design of metamaterial inspired THz antenna

2.1 Antenna design

The aim of this investigation was to develop a metamaterial inspired THz antenna for breast cancer detection. The proposed antenna shown in Fig. 1 comprise a simple rectangular patch antenna with 50Ω inset feeding in front and metamaterial inspired rectangular split ring resonator structure at the back side with width of W_s and length of L_s dimension and a perfect electric conductor (PEC) substrate T_s thickness T_p thickness copper over the substrate. The dimension of the patch antenna given in Table 1.

2.2 Evolution of design

The evolution of antenna design comprises four major steps shown in Fig. 2 in which initially, at step 1 is a simple rectangular patch with the patch length L_p and patch width W_p designed. The length and width of the patch taken for initial consideration since it greatly affects the resonant frequency of the antenna at first step 0.6 THz resonant frequency with the return loss of -11.59 dB along with -10 dB bandwidth of 0.16 THz obtained.

The next step 2 consists of the parametric study for modifying the ground structure for the addition of SRR structure. In step 1 the ground plane consists of gold with L_s length and W_s width and T_g thickness designed for operating in 1 THz frequency. The parameter W_s initially modified and simulation done and there are no major changes found in the antenna. Since the parameter T_g is the thickness of the gold which initially fixed the next parameter is L_s is still available for parametric study. In step 2 the parametric study done with L_s and simulations done by reducing the value to $L_s/2$ and found there is improvement in return loss then G_l found to be the best possible length to obtain -15.62 dB return loss

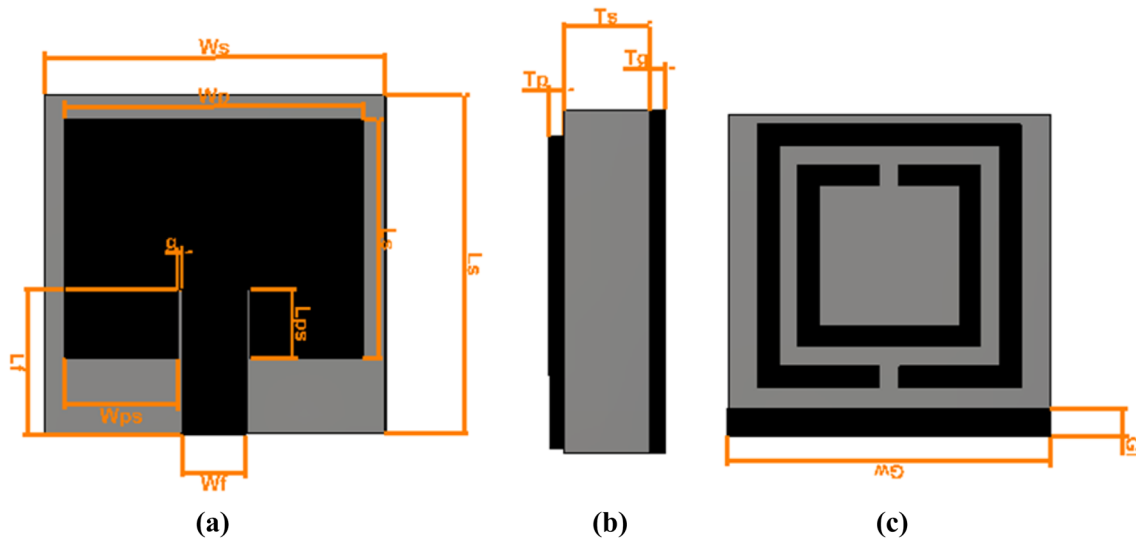


Fig. 1 Proposed antenna with its geometry

Table 1 Dimensions

Parameter	Dimension in nm
Ws	800
Ls	800
Wp	700
Lp	560
Lf	340
Wf	150
g	10
Wps	265
Lps	160
Ts	200
Tp	36
Tg	36
G1	68.55
Gw	800

at 0.65 THz resonant frequency. SRR added in the step 3 which changes the current flow of a rectangular patch and changes the resonant frequencies to 0.8 THz with the return loss of -13 dB along with -10 dB bandwidth of 30 THz respectively. Finally, at step 4 resonant frequency of 1 THz with return loss of -35 dB along with -10 dB bandwidth of 0.37 THz the return loss plot obtained during the evolution of design and parametric study given in Fig. 3.

The CSRR structure used here shown in Fig. 4 and its equivalent circuit with dimensions tabulated in a Table 2.

The performance of metamaterial depends on the material properties retrieved using waveguide-based retrieval method which is effective and robust for measuring the complex permittivity and permeability of metamaterial. A waveguide port in Computer Simulation Technology (CST) is equivalent to the semi-infinite waveguide

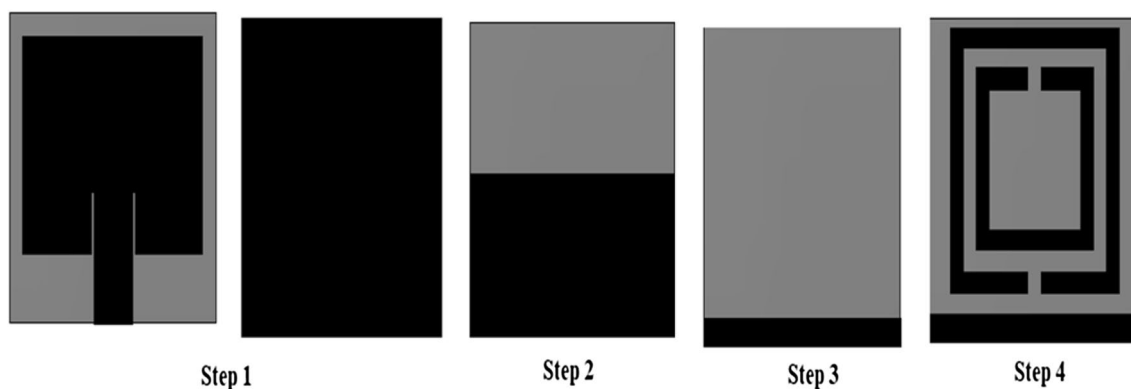


Fig. 2 Evolution of design

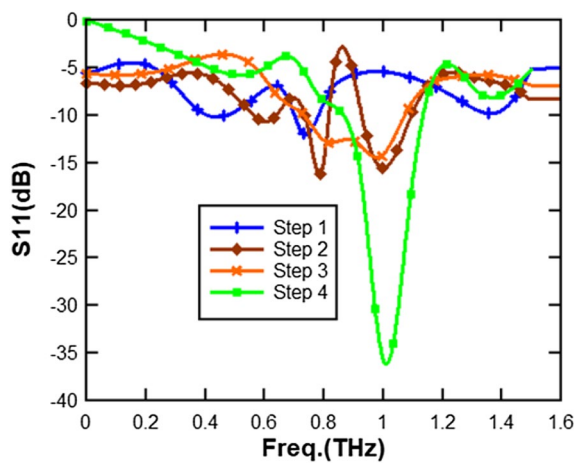


Fig. 3 Return loss observed during evolution process and parametric study

setup which can excite the structure with the incident wave perpendicular to the surface of the port. CSRR analyzed using the waveguide simulation setup shown in Fig. 5.

CSRR can act as a resonant magnetic dipole which can be excited by an axial electric field therefore, a waveguide setup with the height of air box which is 1.5 times of the substrate height for analyzing the metamaterial property of the CSRR. Perfect electric conductor (PEC) and perfect magnetic conductor (PMC) are the symmetric boundaries which used in this simulation of unit cell for creating a periodic boundary condition for analyzing the CSRR. PEC used where the magnetic field is symmetric and an electric field is asymmetric and PMC used where the electric field is symmetric and magnetic field is asymmetric. In this method CSRR kept inside the waveguide medium along xy plane and the perfect electric and magnetic conductor (PEC & PMC) fields placed on the top and bottom of the waveguide along z plane and the electromagnetic field applied its input port 1 and the

Table 2 Dimensions of the CSRR

Parameter	Dimension in nm
Wp, Lp	800
L1	650
L2	450
W1, W2, g	50

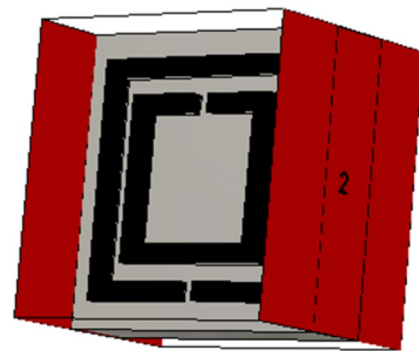


Fig. 5 Waveguide setup of CSRR simulation

corresponding S11 and S21 obtained at the output port 2 and the resonant frequency calculated from the equations given below.

$$f_{CSRR} = \frac{1}{2\pi \sqrt{L_{CSRR} C_{CSRR}}}$$

$$C_{CSRR} = \frac{N-1}{2} [2L - (2N-1)(W+S)] C_0$$

$$C_0 = \epsilon_0 \frac{k(\sqrt{1-k^2})}{k(k)}$$

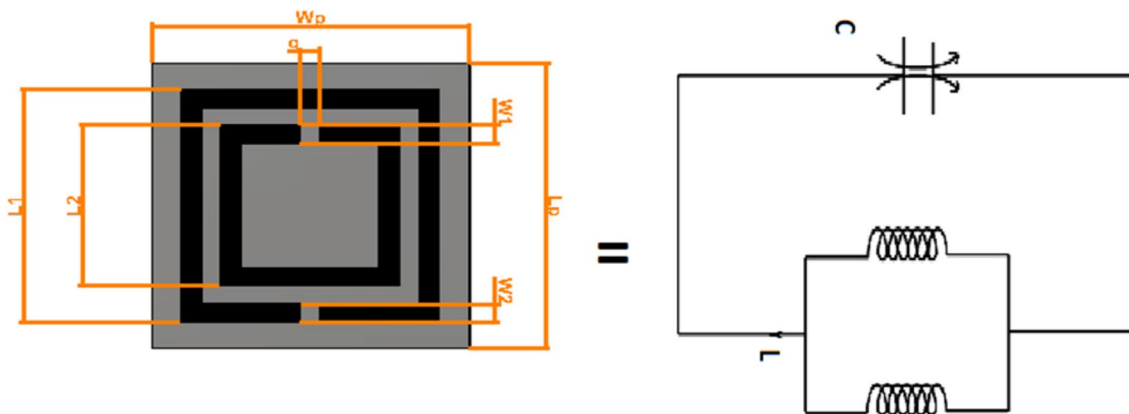


Fig. 4 CSRR along with its equivalent circuit

$$K = \frac{s/2}{w + s/2}$$

$$L_{CSRR} = 4\mu_0[L - (N - 1)(S = W)] \left[\ln \left(\frac{0.98}{\rho} \right) + 1.84\rho \right]$$

$$\rho = \frac{(N - 1)(W + S)}{1 - (N - 1)(W + S)}$$

Here the number of CSRR is 2 and length of the rings L1 and L2 are 650 nm and 450 nm, respectively. Spacing between the slots were 50 nm and the values of capacitance and an inductance of CSRR L_{CSRR} and C_{CSRR} found from the equations, For $N=2$, $L=650$ nm, the f_{CSRR} found as 1 THz.

The negative permittivity versus frequency plot of the CSRR shown in Fig. 6 which calculated using the above equations from that the designed CSRR is resonating exactly at the resonant frequency 1 THz since the real and imaginary part of the permittivity values was overlaps at 1 THz it denotes the resonant frequency of the designed CSRR. The proposed antenna is excited by 50 ohms of impedance micro strip line inset feed since it provides better impedance matching and the dimensions of micro strip line feed is 340 nm length and 150 nm width. In the CST simulation environment, discrete port used for the excitation purpose.

2.3 Performance evaluation

Performance of the proposed metamaterial antenna analyzed in this section. Voltage standing wave ratio (VSWR) an important parameter in antenna design and VSWR for the proposed metamaterial antenna given in Fig. 7 the

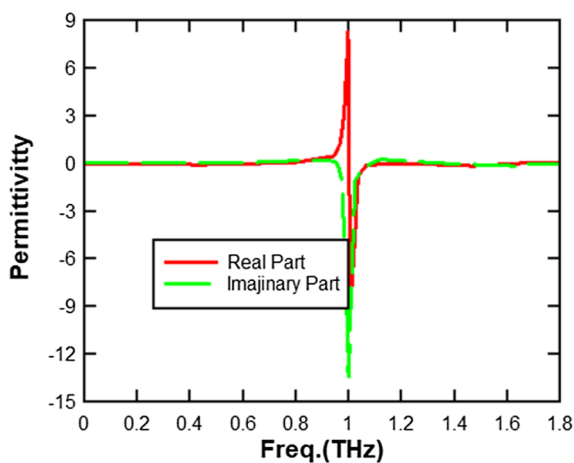


Fig. 6 permittivity versus frequency

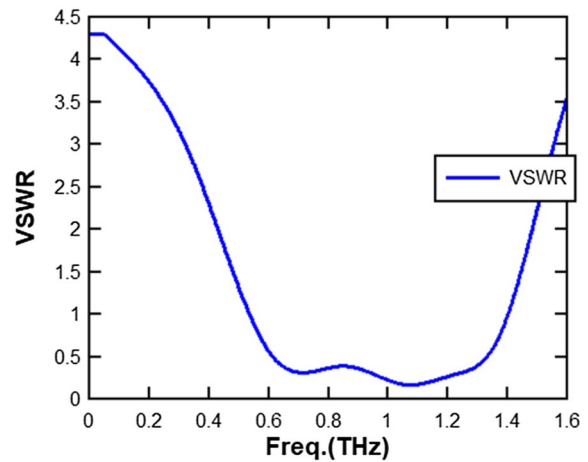


Fig. 7 VSWR of proposed metamaterial antenna

value lies below 0.5 and for the better performance VSWR expected between 0 to 1.5 and the proposed metamaterial antenna satisfies this condition (Fig. 8).

3D farfield pattern obtained from the simulation of the proposed metamaterial antenna given in Fig. 9 at 1 THz resonant frequency shows the proposed antenna achieves 20 dBi of gain and stable radiational characteristics over the entire operating region.

2D farfield pattern analysis plays vital role in performance analysis of any antenna. In Fig. 9 E and H plane of the antenna with and without the addition of metamaterial structure at 1 THz resonant frequency given which clearly shows that the radiational characteristics improved by the addition of the CSRR metamaterial structure. Radiations at both the E plane and H plane are highly becomes directional after the addition of metamaterial structure.

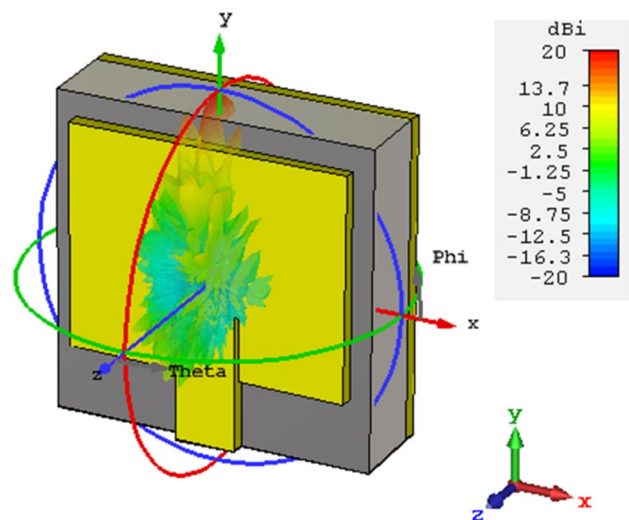


Fig. 8 3D farfield pattern of the metamaterial antenna

Fig. 9 2D Farfield pattern of the metamaterial antenna, **a** antenna without metamaterial, **b** antenna with metamaterial

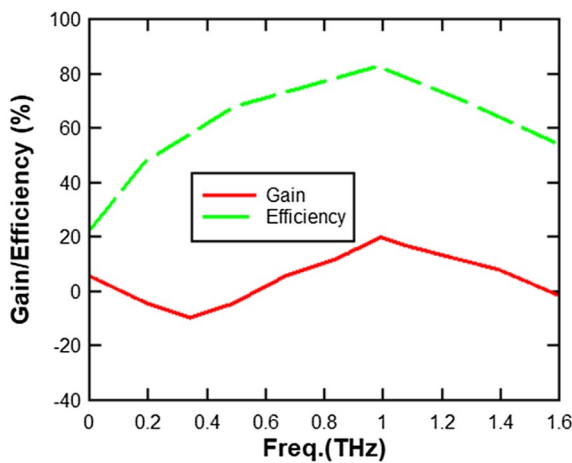
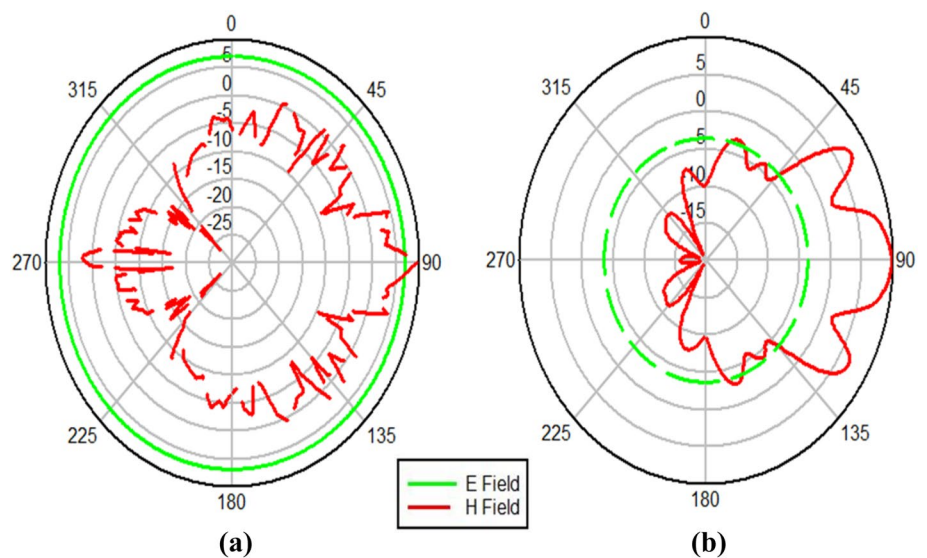


Fig. 10 Gain and efficiency versus frequency of the proposed metamaterial antenna

Gain and Efficiency versus Frequency of the proposed metamaterial antenna given in Fig. 10 shows that the antenna achieved stable gain and efficiency over the operating frequency. Gain of 20 dBi and efficiency of 80% achieved by the proposed metamaterial antenna.

3 Experiment

The experimental setup for the detection of tumor in human breast model done using CST microwave studio. The physical basics of THz based breast cancer detection work as finding the difference between the normal tissue and the malignant tissue by the variation in the dielectric properties of the normal and malignant tissue. The dielectric properties of the skin can be significantly higher than

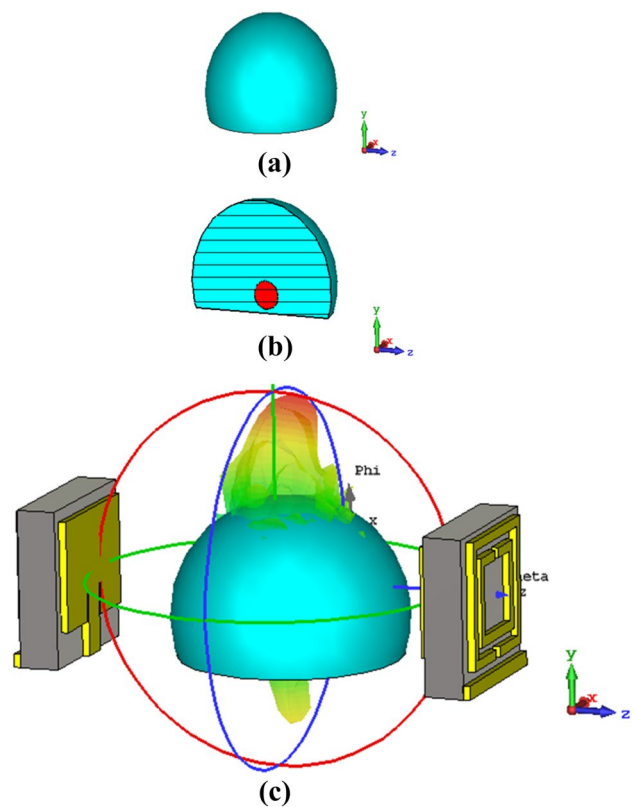


Fig. 11 **a** Human breast model, **b** human breast model along with tumor, **c** breast cancer detection experimental setup

the internal breast tissues generating unwanted reflections and multipath effects [6]. These effects analyzed and the malignant tissue identified with help of the impulse response of the antennas used in this proposed experiment. The human breast model given in Fig. 11a modelled

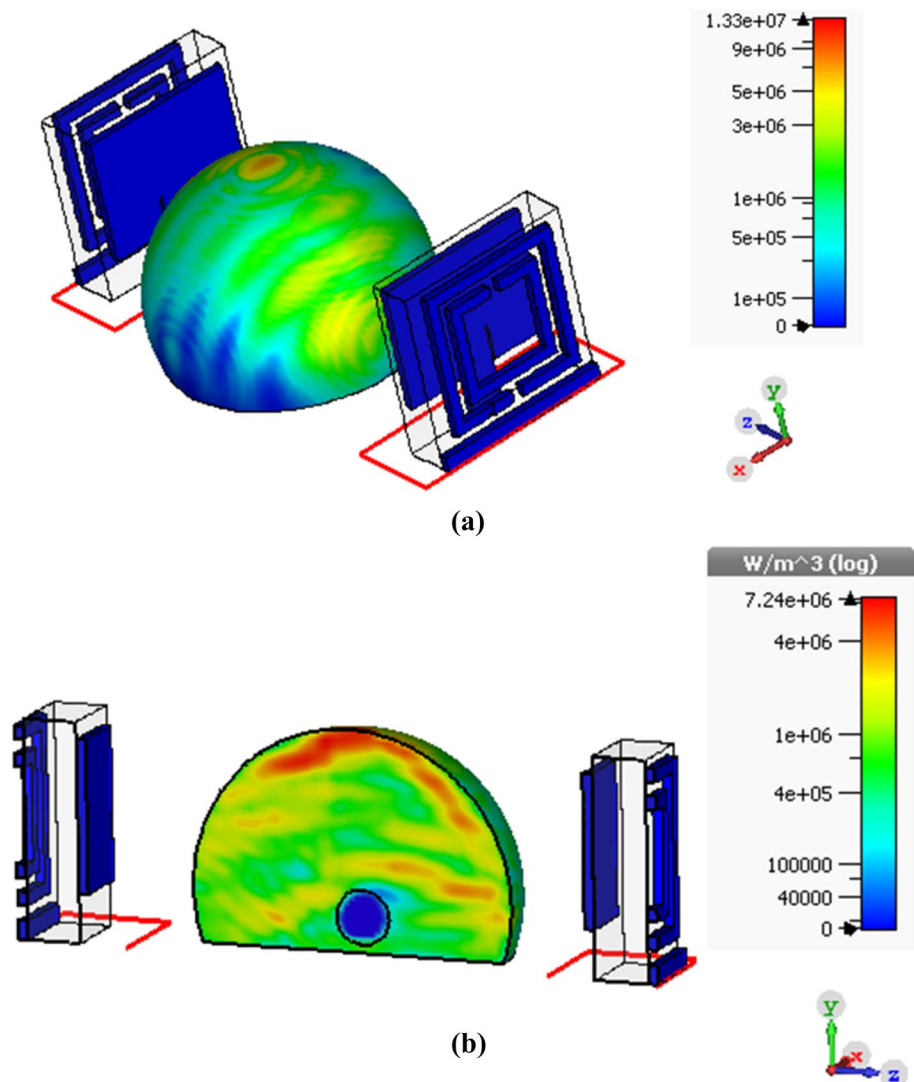
using relative permittivity of 2.41 and the tumor with relative permittivity 3.18 the values of relative permittivity obtained from [31] placed inside the breast model given in Fig. 11b. The experimental setup for detecting tumor in breast tissue given in Fig. 11c. The dimension of the breast sample used in this sample is 800×1200 nm which not followed real dimension since the small sample dimension of breast tissue used here will reduce computational time and resources required for simulation and obtains faster analysis. The two metamaterial antennas act as transmitter (antenna 1) and receiver (antenna 2) antennas placed either side of the breast model along with tumor.

The experiment repeated two times for observing the signal from the breast tissue both with and without tumor for the detection of variation in the signal levels. Figure 12a represents the experimental setup without tumor and Fig. 12b.

In Fig. 12a power pattern without tumor given which shows the uniform distribution of transmitted power over the breast tissue and in Fig. 12b power pattern with tumor given which shows the distribution of power is not even and some power from the radiation absorbed by the tumor and leads to deflections and variation in power distribution obtained.

The input THz signal in time domain is given in Fig. 13a The impulse response obtained from the antenna 2 when normal tissue is given in Fig. 13b and the Fig. 13c shows the response when the normal tissue contains tumor in which the deflections were observed resulting in detection of variation in dielectric constant between the normal tissue and tumor.

Fig. 12 **a** Experimental setup without tumor, **b** experimental setup with tumor



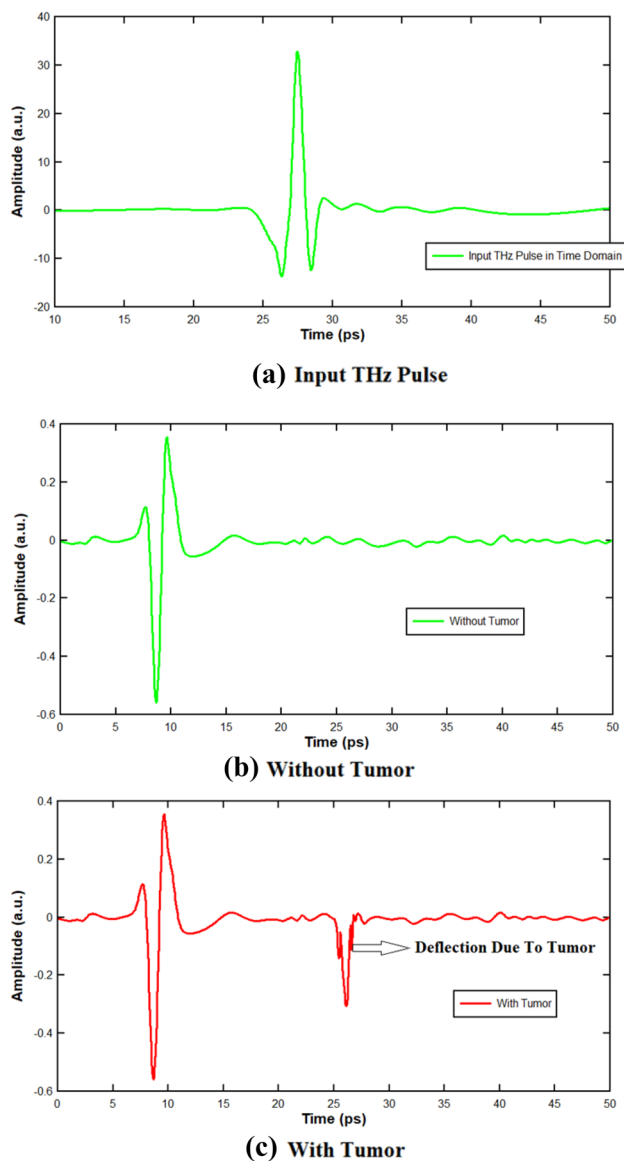


Fig. 13 Tumor detection

4 Conclusion

Breast cancer is a deadly disease becoming widely common these days needs to be detected in its early stages of tumor development for better treatment. This research proposes a novel method for detection of tumor in human breast tissue using metamaterial inspired antenna which operates in THz frequency region. The accuracy of the proposed method is validated by the simulation of the proposed antenna along with human breast phantom model. The experimental technique proposed in this paper clearly shows the detection of tumor in breast tissue model. The accuracy of the proposed model is further improved by improving the performance

characteristics of the proposed metamaterial inspired THz antenna.

Compliance with ethical standards

Conflict of interest The authors declare that they have no conflict of interest.

Human and animal rights The authors declare that there is no human participants and/or animals used in this research

References

1. Welch HG, Prorok PC, O'Malley AJ, Kramer BS (2016) Breast-cancer tumor size, overdiagnosis, and mammography screening effectiveness. *N Engl J Med* 375(15):1438–1447. <https://doi.org/10.1056/nejmoa1600249>
2. Drukteinis JS, Mooney BP, Flowers CI, Gatenby RA (2013) Beyond mammography: new frontiers in breast cancer screening. *Am J Med* 126(6):472–479. <https://doi.org/10.1016/j.amjmed.2012.11.025>
3. Rahmatinia S, Fahimi B (2017) Magneto-thermal modeling of biological tissues: a step toward breast cancer detection. *IEEE Trans Magn* 53(6):1–4. <https://doi.org/10.1109/tmag.2017.2671780>
4. Balaji R, Ramachandran KN (2009) Magnetic resonance imaging of a benign phyllodes tumor of the breast. *Breast Care* 4(3):2–2. <https://doi.org/10.1159/000220604>
5. Porter E, Coates M, Popovic M (2016) An early clinical study of time-domain microwave radar for breast health monitoring. *IEEE Trans Biomed Eng* 63(3):530–539. <https://doi.org/10.1109/tbme.2015.2465867>
6. Byrne D, Sarafianou M, Craddock IJ (2017) Compound radar approach for breast imaging. *IEEE Trans Biomed Eng* 64(1):40–51. <https://doi.org/10.1109/tbme.2016.2536703>
7. Bassi M, Caruso M, Khan MS, Bevilacqua A, Capobianco A-D, Neviani A (2013) An integrated microwave imaging radar with planar antennas for breast cancer detection. *IEEE Trans Microw Theory Tech* 61(5):2108–2118. <https://doi.org/10.1109/tmtt.2013.2247052>
8. Porter E, Kirshin E, Santorelli A, Coates M, Popovic M (2013) Time-domain multistatic radar system for microwave breast screening. *IEEE Antennas Wirel Propag Lett* 12:229–232. <https://doi.org/10.1109/lawp.2013.2247374>
9. Zhang H, El-Rayis AO, Haridas N, Noordin NH, Erdogan AT, Arslan T (2011) A smart antenna array for brain cancer detection. In: 2011 Loughborough antennas and propagation conference. <https://doi.org/10.1109/lapc.2011.6114045>
10. Ouerghi K, Fadlallah N, Smida A, Ghayoula R, Fattahi J, Boulefflen N (2017) Circular antenna array design for breast cancer detection. In: Sensors networks smart and emerging technologies (SENSET). Beirut, pp 1–4. <https://doi.org/10.1109/SENSET.2017.8125016>
11. Asili M, Chen P, Hood AZ, Purser A, Hulsey R, Johnson L, Top-sakal E (2015) Flexible microwave antenna applicator for chemothermotherapy of the breast. *IEEE Antennas Wirel Propag Lett* 14:1778–1781. <https://doi.org/10.1109/lawp.2015.2423655>
12. Mahmud MZ, Islam MT, Rahman MN, Alam T, Samsuzzaman M (2017) A miniaturized directional antenna for microwave breast imaging applications. *Int J Microw Wirel Technol* 9(10):2013–2018. <https://doi.org/10.1017/s1759078717000927>

13. Chandra R, Zhou H, Balasingham I, Narayanan RM (2015) On the opportunities and challenges in microwave medical sensing and imaging. *IEEE Trans Biomed Eng* 62(7):1667–1682. <https://doi.org/10.1109/tbme.2015.2432137>
14. Al-Ibadi A, et al (2017) THz spectroscopy and imaging for breast cancer detection in the 300–500 GHz range. In: 2017 42nd International conference on infrared, millimeter, and terahertz waves (IRMMW-THz), Cancun, pp 1–1. <https://doi.org/10.1109/IRMMW-THz.2017.8067037>
15. Bowman TC, El-Shenawee M, Campbell LK (2015) Terahertz imaging of excised breast tumor tissue on paraffin sections. *IEEE Trans Antennas Propag* 63(5):2088–2097. <https://doi.org/10.1109/tap.2015.2406893>
16. Truong BCQ, Tuan HD, Fitzgerald AJ, Wallace VP, Nguyen HT (2015) A dielectric model of human breast tissue in terahertz regime. *IEEE Trans Biomed Eng* 62(2):699–707. <https://doi.org/10.1109/tbme.2014.2364025>
17. Peter BS, Yngvesson S, Siqueira P, Kelly P, Khan A, Glick S, Karelis A (2013) Development and testing of a single frequency terahertz imaging system for breast cancer detection. *IEEE J Biomed Health Inf* 17(4):785–797. <https://doi.org/10.1109/jbhi.2013.2267351>
18. Kushwaha RK, Karuppanan P, Malviya LD (2018) Design and analysis of novel microstrip patch antenna on photonic crystal in THz. *Phys B* 545:107–112. <https://doi.org/10.1016/j.physb.2018.05.045>
19. Yang L, Shi X, Chen K, Fu K, Zhang B (2013) Analysis of photonic crystal and multi-frequency terahertz microstrip patch antenna. *Phys B* 431:11–14. <https://doi.org/10.1016/j.physb.2013.08.036>
20. Malhotra I, Jha KR, Singh G (2018) Terahertz antenna technology for imaging applications: a technical review. *Int J Microw Wirel Technol* 10(03):271–290. <https://doi.org/10.1017/s175907871800003x>
21. Veselago VG (1968) The electrodynamics of substances with simultaneously negative values of ϵ and μ . *Phys Usp* 10(4):509–514
22. Baena JD, Bonache J, Martin F, Sillero RM, Falcone F, Lopetegui T, Laso MAG, Garcia-Garcia J, Gil I, Portillo MF, Sorolla M (2005) Equivalent-circuit models for split-ring resonators and complementary split-ring resonators coupled to planar transmission lines. *IEEE Trans Microw Theory Tech* 53(4):1451–1461. <https://doi.org/10.1109/tmmt.2005.845211>
23. Singh R, Smirnova E, Taylor AJ, O'Hara JF, Zhang W (2008) Optically thin terahertz metamaterials. *Opt Express* 16(9):6537. <https://doi.org/10.1364/oe.16.006537>
24. Choudhury M, Bisoyi S, Reddy PV, Manjula S (2014) Emerging trends in terahertz metamaterial applications. *CMC Comput Mate Continua*, 39(3): 179–215. <https://doi.org/10.3970/cmc.2014.039.179>
25. Epstein NR, Meaney PM, Paulsen KD (2014) 3D parallel-detection microwave tomography for clinical breast imaging. *Rev Sci Instrum* 85(12):124704
26. A. W. Preece, I. J. Craddock, M. Shere, L. Jones, and H. L. Winton, MARIA M4: Clinical evaluation of a prototype ultrawideband radar scanner for breast cancer detection, *Journal of Medical Imaging*, 3(3), 033502, 2016.29.
27. Bourqui J, Kuhlmann M, Kurrant DJ, Lavoie BR, Fear EC (2018) Adaptive monostatic system for measuring microwave reflections from the breast. *Sensors* 18(5):1340
28. Fear EC, Bourqui J, Curtis C, Mew D, Docktor B, Romano C (2013) Microwave breast imaging with a monostatic radar-based system: a study of application to patients. *IEEE Trans Microw Theory Tech* 61(5):2119–2128
29. Song H, Kono H, Seo Y, Azhari A, Somei J, Suematsu E, Watarai Y, Ota T, Watanabe H, Hiramatsu Y, Toya A, Xiao X, Kikkawa T (2015) A radar-based breast cancer detection system using CMOS integrated circuits. *IEEE Access* 3:2111–2121
30. Song H, Sasada S, Kadoya T, Okada M, Arihiro K, Xiao X, Kikkawa T (2017) Detectability of breast tumor by a hand-held impulse-radar detector: performance evaluation and pilot clinical study. *Sci Rep* 7(1):16353
31. Hidayat MV, Apriono C (2019) Simulation of terahertz imaging using microstrip linear array antenna for breast cancer detection. In: AIP conference proceedings, vol 2092, pp 020020
32. Yu C, Fan S, Sun Y, Pickwell-Macpherson E (2012) The potential of terahertz imaging for cancer diagnosis: a review of investigations to date. *Quant Imaging Med Surg* 2:33–45. <https://doi.org/10.3978/j.issn.2223-4292.2012.01.04>
33. Lazebnik M, Popovic D, McCartney L, Watkins CB, Lindstrom MJ, Harter J, Sewall S, Ogilvie T, Magliocco A, Breslin TM, Temple W, Mew D, Booske JH, Okoniewski M, Hagness SC (2007) A large-scale study of the ultrawideband microwave dielectric properties of normal, benign and malignant breast tissues obtained from cancer surgeries. *Phys Med Biol* 52(20):6093–6115
34. Sugitani T, Kubota S, Kuroki S, Sogo K, Arihiro K, Okada M, Kadoya T, Hide M, Oda M, Kikkawa T (2014) Complex permittivities of breast tumor tissues obtained from cancer surgeries. *Appl Phys Lett* 104(25):253702
35. Martellosio A, Pasian M, Bozzi M et al (2017) Dielectric properties characterization from 0.5 to 50 GHz of breast cancer tissues. *IEEE Trans Microw Theory Tech* 65(3):998–1011

Publisher's Note Springer Nature remains neutral with regard to jurisdictional claims in published maps and institutional affiliations.